Supplementary Information

FGFR3 oncogenic activation drives oxidative metabolic reprogramming in bladder cancer: a systems metabolomics approach

Giacomo Ducci, Giorgia Ciufolini, Gloria Campioni, Valentina Pasquale, Giulia Gigliotti, Simone Ponzetto, Daniele Benedetti, Bruno Giovanni Galuzzi, Deborah D'Aliberti, Silvia Spinelli, Vrunda Satasiya, Elisa Ventura, Chiara Raggi, Riccardo Vago, Marcella Bonanomi, Daniela Gaglio, Antonio Giordano, Andrea Morrione, Chiara Damiani, Rocco Piazza, Daniel Oscar Cicero, Marco Vanoni, Greta Petrella and Elena Sacco

List of supplementary information: Supplementary Figure 1: Morphologic and functional parameters obtained on the UBC cell line panel. **Supplementary Figure 2**: Metabolic parameters obtained on the UBC cell line panel. **Supplementary Figure 3**: Metabolic parameters obtained on the UBC cell line panel using metabolomic analyses. **Supplementary Figure 4**: A computational analysis performed on transcriptomic data from the CCLE cell lines database corroborates experimental results on cell lines. **Supplementary Figure 5**: Mapping of RASs from transcriptomic data of the UBC cell line panel. **Supplementary Figure 6**: OXPHOS targeting in *FGFR3*-altered cell lines. **Supplementary Figure 7**: FCCP dose-response curve and map for INTEGRATE model. **Supplementary Table 1:** Main features of the cell lines under study. **Supplementary Table 2**: List of the detected metabolites detected with NMR analysis.

Supplementary Figure 1

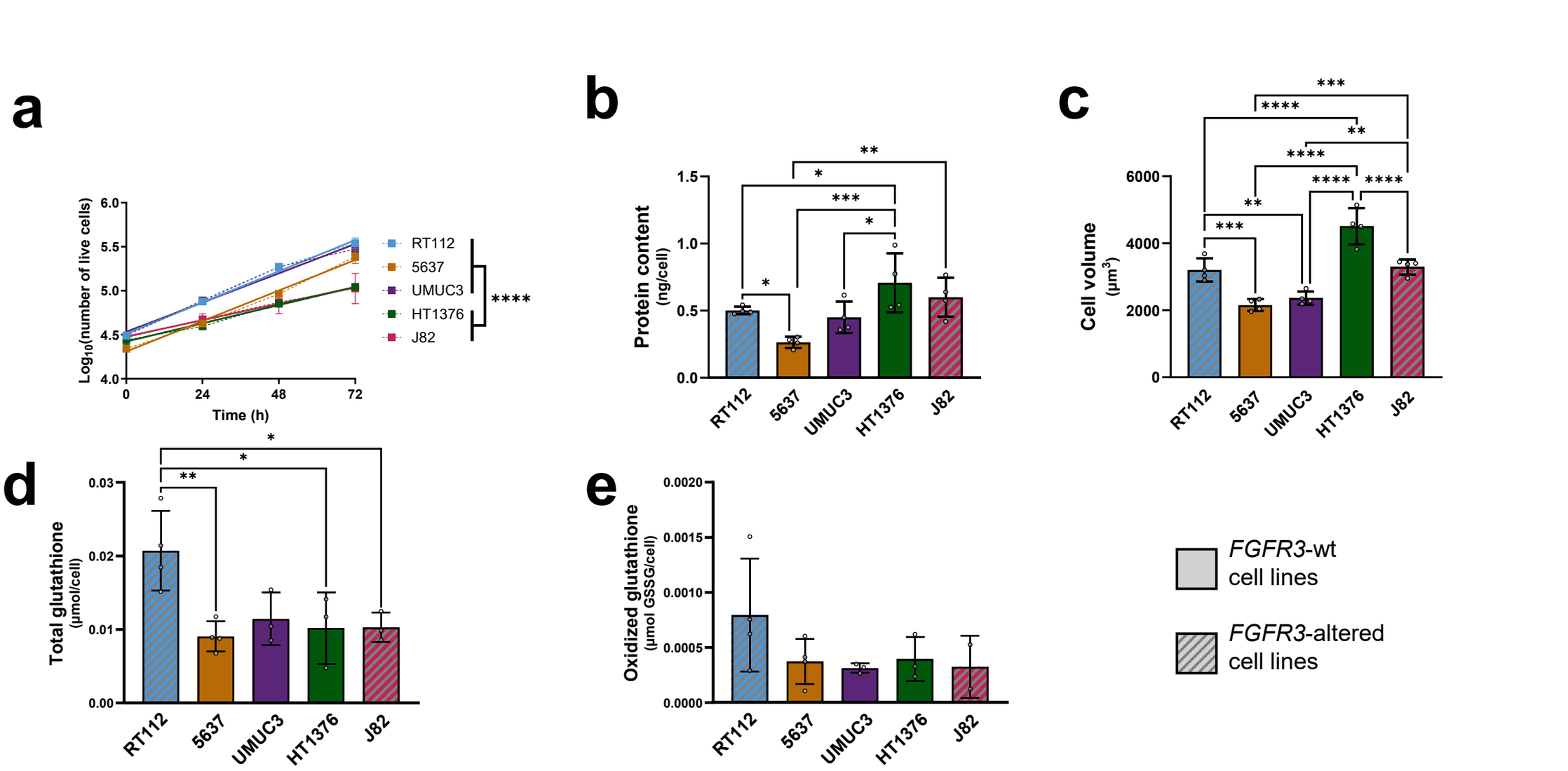

Supplementary Figure 1 Morphologic and functional parameters obtained on the UBC cell line panel. Cell lines presenting an alteration in *FGFR3* are marked with diagonal lines. **(a)** Growth kinetics profiles. **(b)** Cell protein content. **(c)** Cell volume. **(d,e)** Total (d) and oxidized (e) glutathione levels. All the results are shown as mean ± standard deviation. Results are the mean of 2-4 experimental replicates and a total of 4-12 technical replicates. Statistical test: ordinary one-way ANOVA, * for $p < 0.05$; ** for $p < 0.01$; *** for $p < 0.001$; **** for $p < 0.0001$.

Supplementary Figure 2

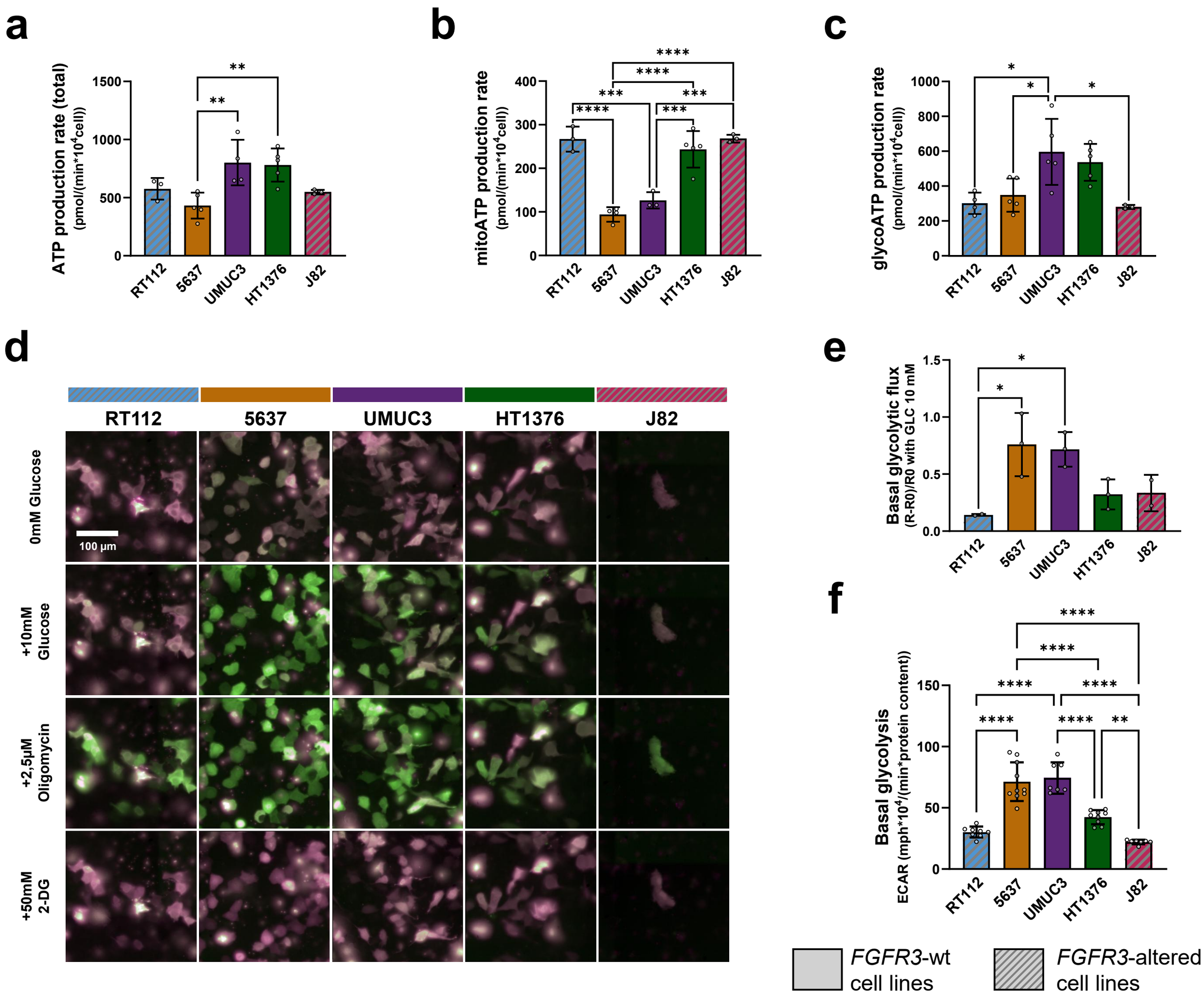

Supplementary Figure 2 Metabolic parameters obtained on the UBC cell line panel. (a-c) Metabolic parameters measured using Seahorse technology: total ATP (a), mitoATP (b), and glycoATP (c) production rates. **(d)** Representative images of cells transfected with Hylight Biosensor, a fluorescent biosensor for fructose 1,6-bisphosphate (FBP), under baseline condition and after the sequential addition of glucose 10mM, oligomycin 2.5 µM and 2-Deoxy-D-glucose (2-DG) 50 mM. Scale bar is 100 µm. **(e)** Basal glycolytic flux using Hylight Biosensor measured as $(R_{GLC} - R_0)/R_0$, where R_{GLC} is the ratio of mean fluorescence intensity of the Hylight biosensor at ex 488 nm / ex 405 nm ($R = F_{488}/F_{405}$) after the pulse of glucose 10 mM, and R_0 is the same ratio calculated at 0 mM glucose (baseline). **(f)** Basal glycolysis measured using Seahorse technology, normalizing data for protein content. All the results are shown as mean ± standard deviation. Results are the mean of 3-5 experimental replicates and a total of 18-50 technical replicates (a-c); 2-3 experimental replicates and a total of 7-17 technical replicates (e). Statistical test: ordinary one-way ANOVA, * for $p < 0.05$; ** for $p < 0.01$; *** for $p < 0.001$; **** for $p < 0.0001$.

Supplementary Figure 3

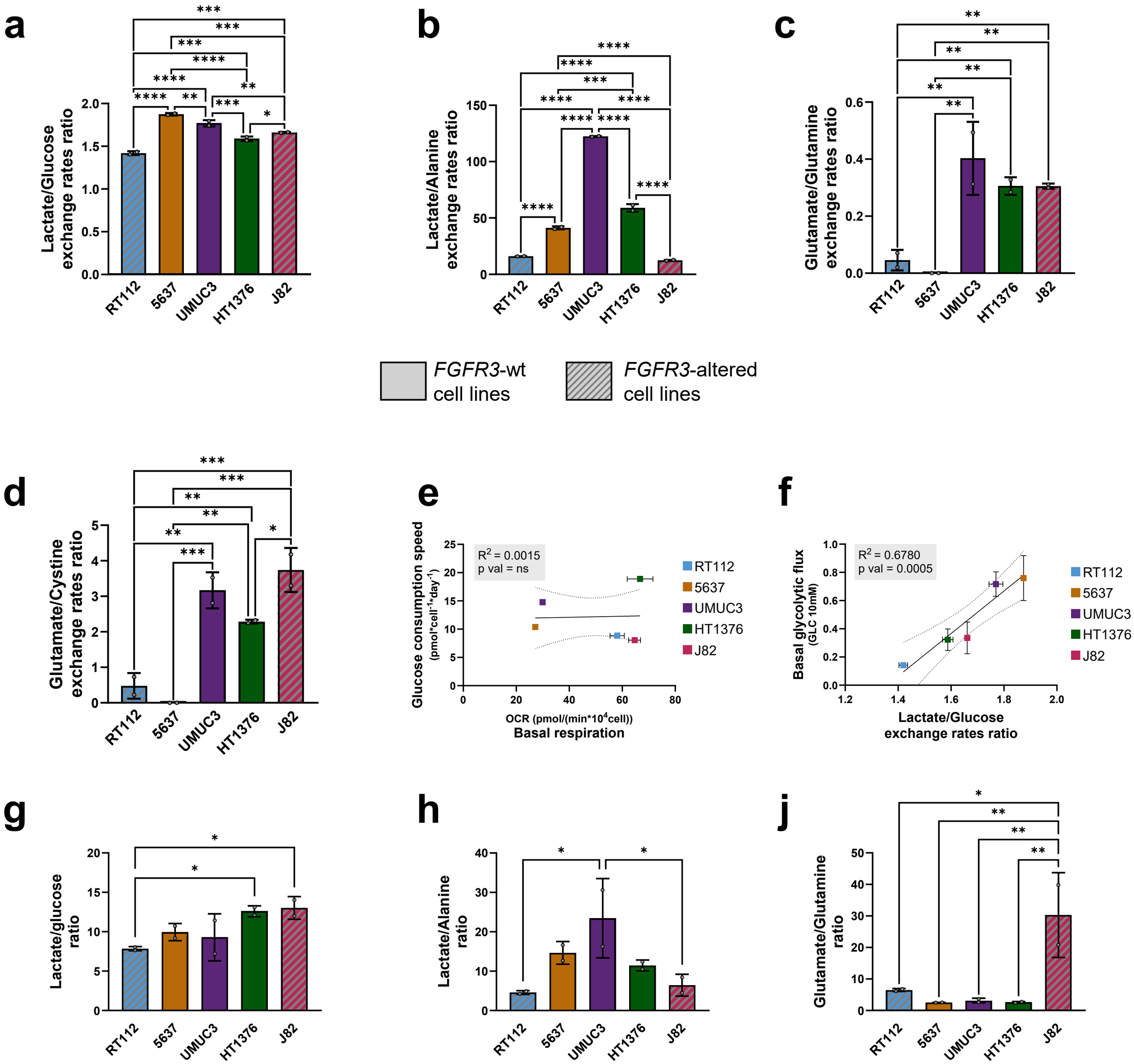

Supplementary Figure 3 Metabolic parameters obtained on the UBC cell line panel using metabolomic analyses. (a-d) Ratios of exchange rates of metabolites detected with NMR analysis (exo-metabolomics): lactate/glucose (a), lactate/alanine (b), glutamate/glutamine (c), glutamate/cystine (d). **(e)** Linear regression analysis between basal respiration from Seahorse technology and glucose consumption from exometabolomics. **(f)** Linear regression analysis between the ratio of the exchange rates of lactate and glucose measured with NMR and basal glycolytic flux measured through Hylight Biosensor after addition of 10mM glucose. **(g-j)** Ratios of intracellular levels of metabolites from LC-MS analysis (endo-metabolomics): lactate/glucose (g), lactate/alanine (h), glutamate/glutamine (j). All the results are shown as mean ± standard deviation. Results are the mean of 2 experimental replicates and a total of 6 technical replicates (a-d, g-j). Statistical test: ordinary one-way ANOVA, * for $p < 0.05$; ** for $p < 0.01$; *** for $p < 0.001$; **** for $p < 0.0001$.

Supplementary Figure 4

a

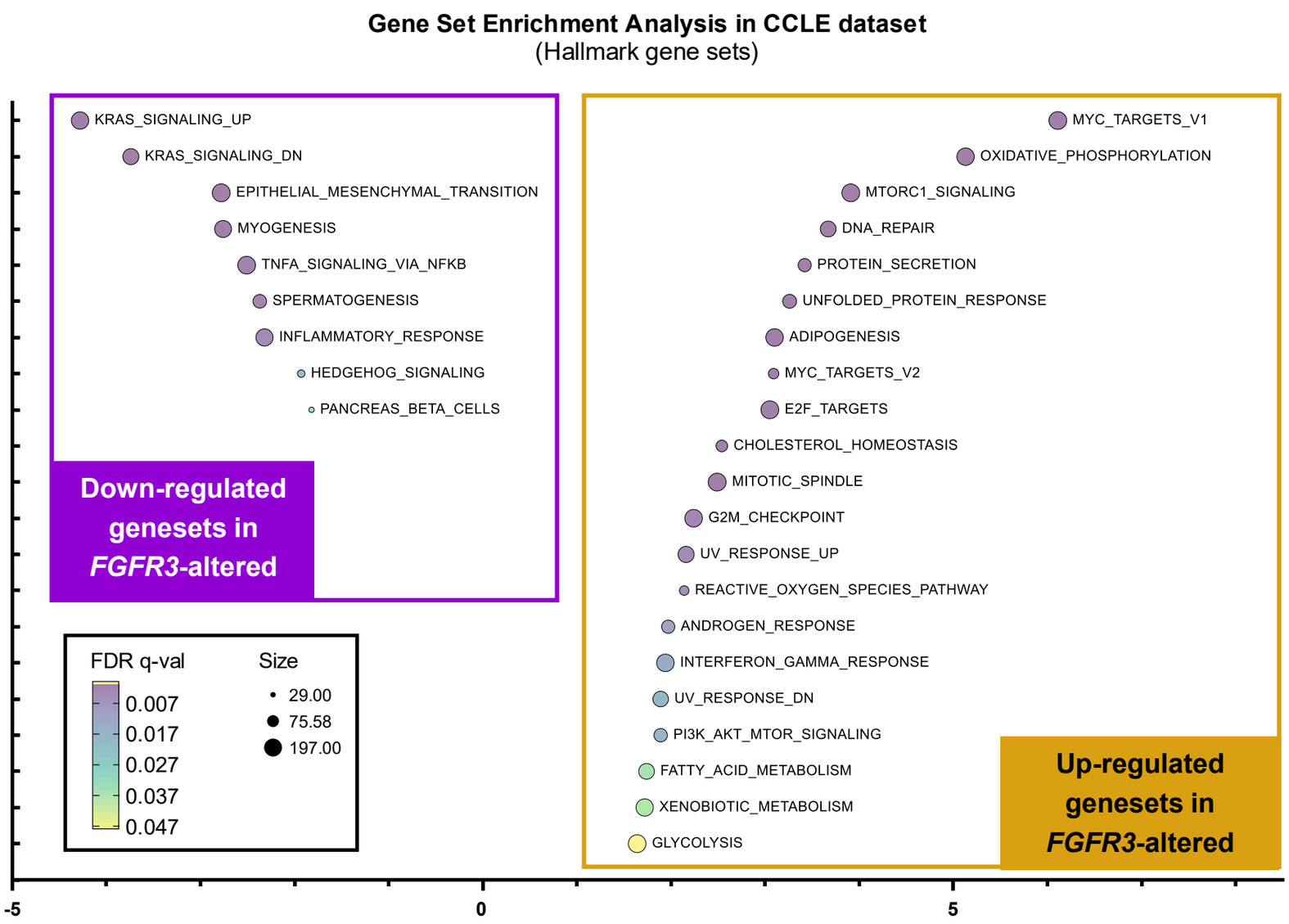

b

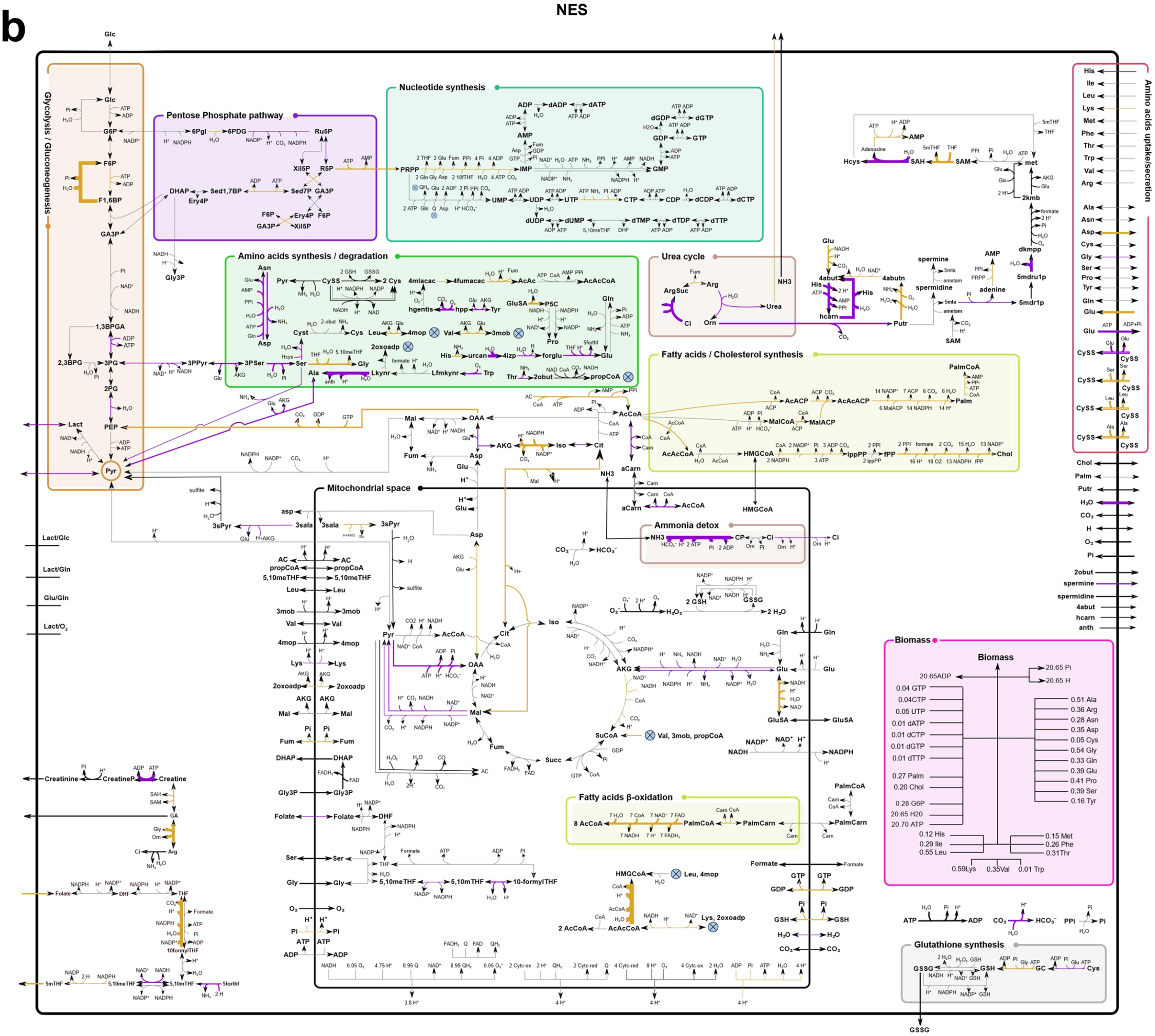

Supplementary Figure 4 A computational analysis performed on transcriptomic data from the CCLE cell lines database corroborates experimental results on cell lines. (a) Gene Set Enrichment Analysis (GSEA) on transcriptomic data using the 50 Hallmark gene sets. Significative gene sets were selected for an FDR q-val < 5% and ordered for Normalized Enrichment Score (NES). **(b)** Mapping of RASs using ENGRO2 model. Purple and yellow arrows represent respectively down-regulated and up-regulated reactions in the *FGFR3*-altered compared to the *FGFR3*-wt group, setting fold-change > 1.2 as threshold.

Supplementary Figure 5

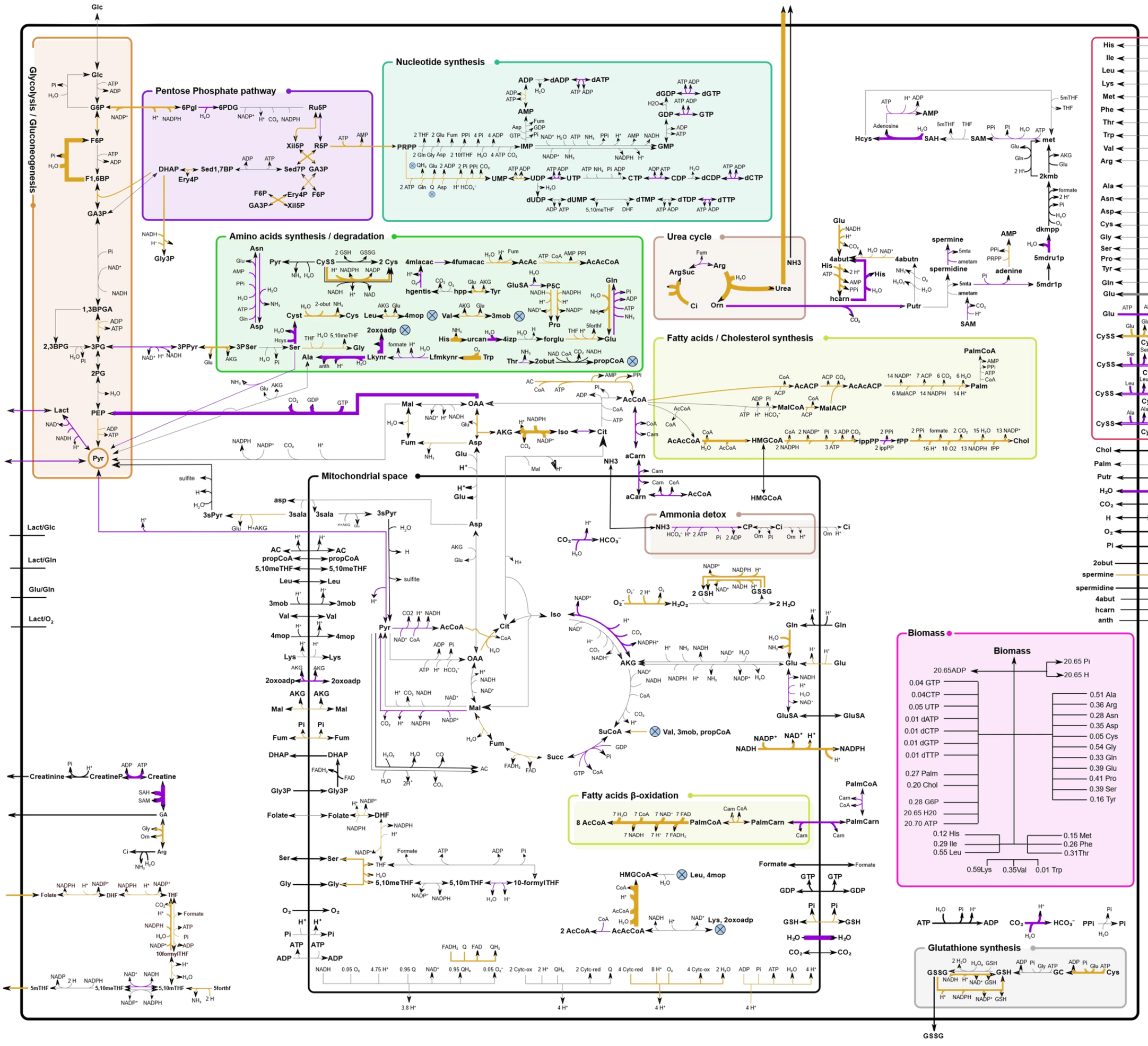

= Down-regulated in *FGFR3*-altered

= Up-regulated in *FGFR3*-altered

Arrow thickness is proportional to z-score

Supplementary Figure 5 Mapping of RASs from transcriptomic data of the UBC cell line panel. RASs were obtained using ENGRO2 model from transcriptomic data of the cell line panel, and filtered setting fold-change > 1.2 as threshold. Purple and yellow arrows represent respectively down-regulated and up-regulated reactions in the *FGFR3*-altered compared to the *FGFR3*-wt group.

Supplementary Figure 6

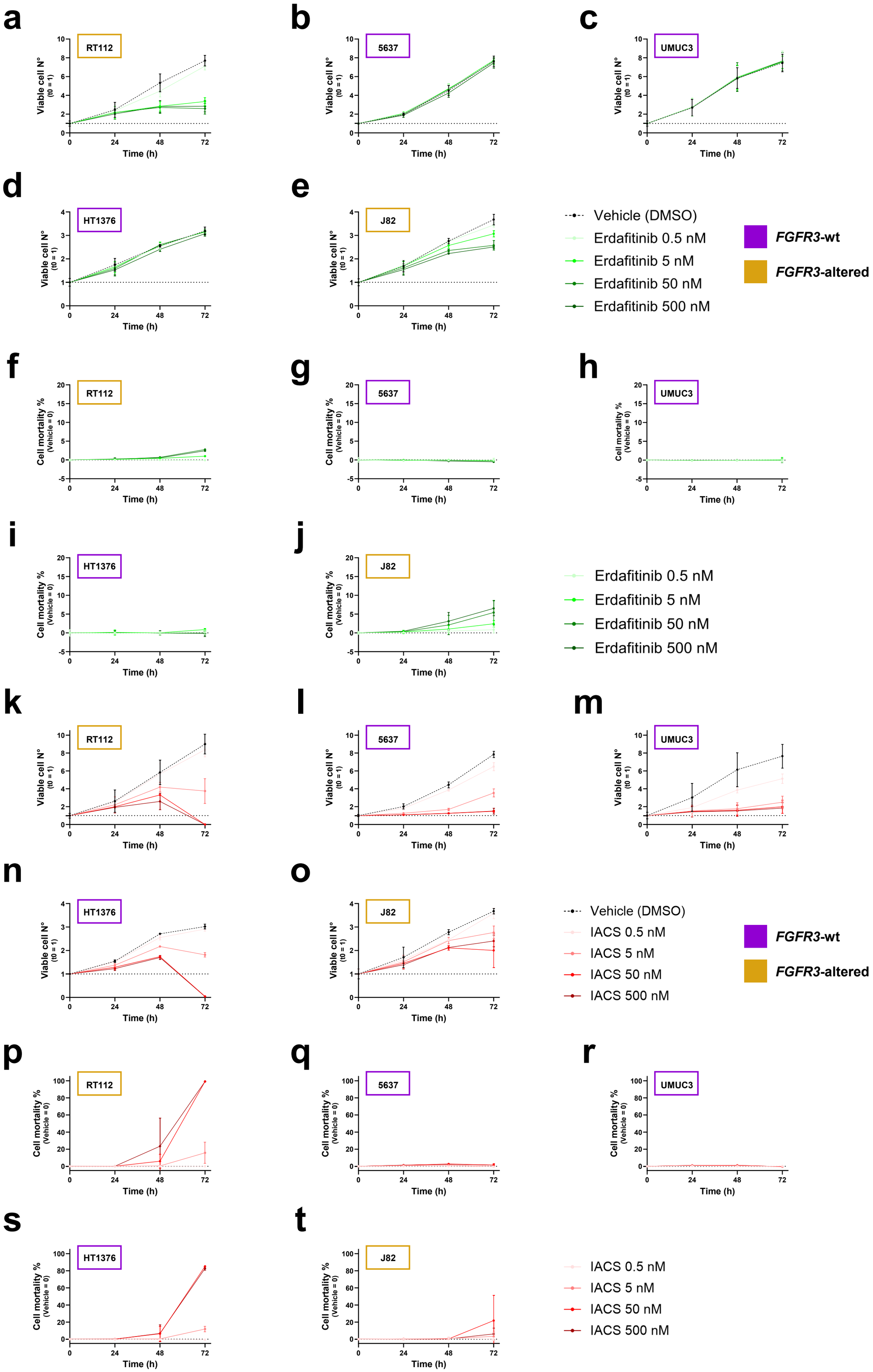

Supplementary Figure 6 FGFR3 and OXPHOS pharmacological inhibition in UBC cell lines. Treatment at 0 to 72h at increasing concentrations (0,5, 5, 50, 500 nM) of the FGFR3 inhibitor Erdafitinib (a-j) or ETC complex I inihibitor IACS-010759 (k-t), showing viable cell count (a-e, k-o) and cell mortality % (f-j, p-t). All the results are shown as mean ± standard deviation.

Supplementary Figure 7

a

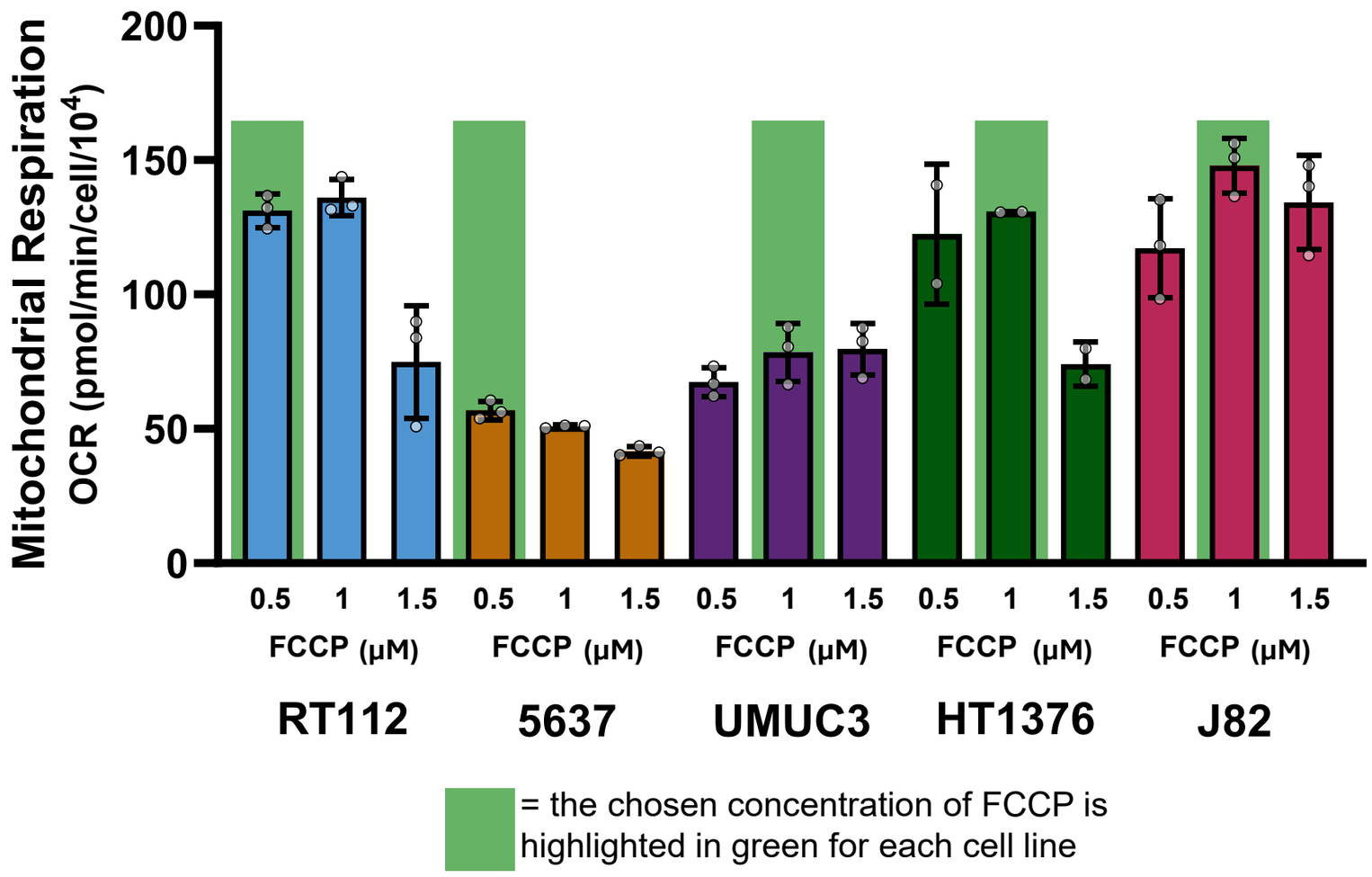

b

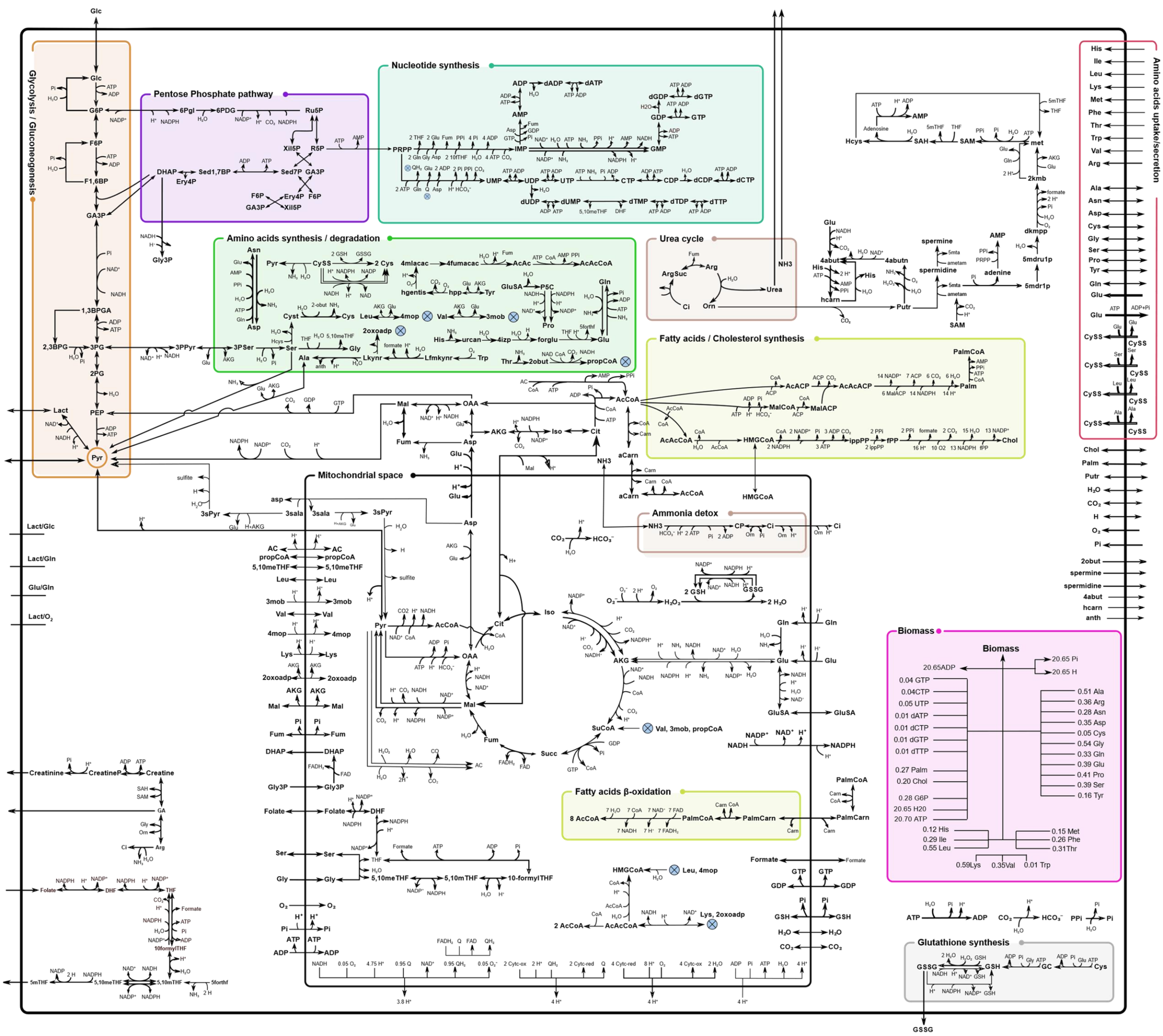

Supplementary Figure 7 FCCP dose-response curve and map for INTEGRATE model. (A) Dose-response curve with FCCP for the determination of maximal respiration parameter (lowest concentration with the highest response). 0.5 μM was chosen for RT112 and 5637 cell lines, while 1 μM was chosen for UMUC3, HT1376 and J82 cell lines (highlighted in green in the graph). All the results are shown as mean ± standard deviation. **(B)** Manually-curated map for visualization of RAS and fluxes predictions obtained using the computational model.

Supplementary Table 1

Color	Cell line	Origin	Stage	Grade	Karyotype	Genetic alterations
	RT112	UBUC	NMIBC (pT<2)	Low grade (G2)	44-47 chromosomes	***FGFR3-TACC3* (gene fusion)**; *TERT* (mutation); *TP53* (heterozygous mutation)
	5637	UBUC	MIBC (pT2)	Low grade (G2)	59-71 chromosomes	*MAPK1* (heterozygous mutation); *RB1* (homozygous mutation); *TERT* (mutation); *TP53* (homozygous mutation)
	UMUC3	UBUC	MIBC (pT>2)	High grade (G3)	78-80 chromosomes	*CDKN2A* (homozygous deletion); *PTEN* (homozygous deletion); *ATM* (heterozygous mutation); *KRAS* (homozygous mutation); *PARD3B* (homozygous mutation); *TERT* (mutation); *TP53* (homozygous mutation)
	HT1376	UBUC	MIBC (pT>2)	High grade (G3)	104-121 chromosomes	*RB1* (homozygous mutation); *TERT* (mutation); *TP53* (mutation)
	J82	UBUC	MIBC (pT3)	High grade (G3)	Hyperdiploid to hexaploid	***FGFR3* (mutation K652E)**; *APC* (heterozygous mutation); *PIK3CA* (heterozygous mutation); *PTEN* (homozygous mutation); *RB1* (homozygous mutation); *TERT* (mutation); *TP53* (heterozygous / homozygous mutation)

Supplementary Table 1 Main features of the cell lines under study. Origin: urinary bladder urothelial carcinoma (UBUC). Stage represents the invasiveness degree of a tumor, namely how it spread into the surrounding tissues and organs: non-muscle-invasive bladder cancer (NMIBC) or muscle-invasive bladder cancer (MIBC). Grade represents the differentiation degree of cells within a tumor (G1 well differentiated, G2 moderately differentiated, G3 poorly differentiated).

Supplementary Table 2

Metabolite	Abbreviation	Consumption/Excretion/Mixed	Assignement	^{1}H n (ppm)	Chemical/Biochemical class
Alanine	Ala	E	CH_3	1.468	Amino Acid and derivative
			CH-α	3.778	
Arginine	Arg	M	CH-α	3.758	
			CH_2-β	1.919	
			CH_2-γ	1.681	
			CH_2-δ	3.233	
Aspartate	Asp	E	CH_2-β	2.671, 2.799	
Cystine	Cys	C	CH-α	4.089	
			CH_2-β	3.174, 3.369	
Glutamate	Glu	M	CH-α	3.731	
			CH_2-β	2.087	
			CH_2-γ	2.339	
Glutamine	Gln	C	CH-α	3.749	
			CH_2-β	2.123	
			CH_2-γ	2.449	
Glycine	Gly	M	CH_2	3.551	
Histidine	His	C	CH-α	3.990	
			CH_2-β	3.256, 3.297	
			CH-δ2	7.122	
			CH-ε1	7.967	
Lysine	Lys	C	CH-α	3.767	
			CH_2-β	1.899	
			CH_2-γ	1.426, 1.488	
			CH_2-δ	1.716	
			CH_2-ε	3.015	
Methionine	Met	C	CH-α	3.847	
			CH_2-β	2.186, 2.109	
			CH_2-γ	2.631	
			CH_3-ε	2.126	
Ornithine	Orn	M	CH_2-δ	3.046	
Serine	Ser	C	CH-α	3.840	
			CH_2-β	3.956, 3.979	
Threonine	Thr	M	CH_3-γ	1.317	
			CH-β	4.254	
			CH-α	3.588	
Phenylalanine	Phe	M	CH-δ	7.319	
			CH-ε	7.419	
			CH-ζ	7.367	
Tyrosine	Tyr	C	CH-δ	7.175	
			CH-ε	6.862	
Sarcosine	Sar	M	CH_3	2.730	
			CH_2	3.610	
Pyroglutamate	Pyro	M	CH-α	4.169	
			CH_2-β	2.025, 2.496	
			CH_2-γ	2.393	
2-Phenylpropionate	2PheProp	E	CH-α	3.650	Aromatic Compound
			CH_3-β	1.420	
Isoleucine	Ile	C	CH_3-δ	0.933	Branched-Chain Amino Acid
			CH_3-γ2	0.997	
Leucine	Leu	C	CH_3-δ1	0.948	
			CH_3-δ2	0.958	
Valine	Val	C	CH_3-γ1	1.038	
			CH_3-γ2	0.984	
			CH-β	2.251	
			CH-α	3.606	
Fructose	Fruc	M	αCH-1	4.105	Energy Metabolite
			βCH-1	3.789	
			αCH -2	4.106	
			βCH-2	3.879	
			βCH-3	3.992	
Glucose	Gluc	C	αCH -1	5.227	
			βCH-1	4.606	
			αCH -2	3.530	
			βCH-2	3.238	
			αCH -3	3.697	
			βCH-3	3.469	
			αCH -4	3.403	
			βCH-4	3.403	
			αCH -5	3.808	
			βCH-5	3.469	
			αCH_2-6	3.828	
			βCH_2-6	3.732, 3.887	
Creatine	Cr	M	CH_3	3.030	
			CH_2	3.930	
Creatinine	Crea	M	CH_3	3.020	
			CH_2	4.030	
Lactate	Lact	E	CH_3	1.317	Glycolytic Metabolite
			CH	4.106	
Pyruvate	Pyr	M	CH_3	2.364	
Formate	For	E	CH	8.451	One-Carbon Metabolite
Dimethyl sulfone	DMS	M	CH_3	3.04	Organosulfur Compound
Myo-inositol	Ino	M	CH-1	4.059	Polyol
			CH-2	3.628	
			CH-4	3.282	
Choline	Ch	C	CH_3	3.179	Quaternary Amine
			N-CH_2	3.508	
Acetate	Ala	M	CH_3	1.920	Short-chain Fatty Acid
2-Oxoglutarate	2OXG	E	CH_2-β	2.950	TCA Cycle Intermediate
			CH_2-γ	2.400	
Citrate	Cit	E	CH_2	2.520, 2.680	
Fumarate	Fum	E	CH	6.509	
Succinate	Suc	M	CH_2–CH_2	2.400	
Pantothenate	Panto	M	CH_2	3.550	Vitamins
			CH_2-CONH	2.450	
			CH-OH	4.050	
			CH_3	0.900	
Pyridoxine	Pyrid	C	CH_2	4.700-4.900	
			CH	7.950	
			CH_3	2.650	
Niacinamide	Niac	C	OCC-CH-N	9.040	
			CH-N	8.751	

Supplementary Table 2 List of the detected metabolites detected with NMR analysis. Metabolites identified in the extracellular media of BC cell lines based on their flux behavior—Consumption (C), Excretion (E), or Mixed Behavior (M)—as determined by NMR-based exometabolomics analysis, with their chemical shifts (δ, ppm).